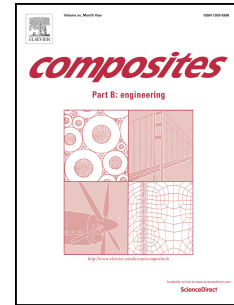


# Accepted Manuscript

Experimental assessment of the mechanical behaviour of 3D woven composite T-joints

Shibo Yan, Xuesen Zeng, Andrew Long



PII: S1359-8368(18)30445-1

DOI: [10.1016/j.compositesb.2018.08.007](https://doi.org/10.1016/j.compositesb.2018.08.007)

Reference: JCOMB 5837

To appear in: *Composites Part B*

Received Date: 11 April 2018

Revised Date: 25 June 2018

Accepted Date: 2 August 2018

Please cite this article as: Yan S, Zeng X, Long A, Experimental assessment of the mechanical behaviour of 3D woven composite T-joints, *Composites Part B* (2018), doi: 10.1016/j.compositesb.2018.08.007.

This is a PDF file of an unedited manuscript that has been accepted for publication. As a service to our customers we are providing this early version of the manuscript. The manuscript will undergo copyediting, typesetting, and review of the resulting proof before it is published in its final form. Please note that during the production process errors may be discovered which could affect the content, and all legal disclaimers that apply to the journal pertain.

# Experimental assessment of the mechanical behaviour of 3D woven composite T-joints

Shibo Yan<sup>1</sup>, Xuesen Zeng<sup>2</sup> and Andrew Long<sup>1</sup>

<sup>1</sup> Composites Research Group, Faculty of Engineering, University of Nottingham, Nottingham NG7 2RD, UK

<sup>2</sup> Centre for Future Materials, University of Southern Queensland, Toowoomba 4350, Queensland, Australia

## Abstract

To understand the influence of the fibre architecture of 3D woven composite T-joints on mechanical performance, as well as the benefits that 3D woven T-joints can offer over the equivalent 2D laminates, experimental testing is performed on two types of 3D woven T-joint with only weave variation at the junction, and one type of 2D woven laminate T-joint. A quasi-static tensile pull-off loading is selected in this work as this out-of-plane load case is one of the typical loading conditions for such T-joint structures. The significant advantages of 3D woven composite T-joints in terms of ultimate strength and damage tolerance over the 2D alternative were identified in the testing. More importantly, this work showed that variation in the fibre architecture can considerably enhance properties such as delamination resistance and total energy absorption to failure, as well as increasing slightly the stiffness and initial failure load. This experimental assessment has demonstrated that using 3D woven reinforcements is an effective way to improve the load-bearing capability of composite T-joints over laminates, and also that this improvement could be optimised with regard to fibre architecture.

Keywords: A. 3-Dimensional reinforcement; B. Mechanical properties; B. Damage tolerance; D. Mechanical testing

## 1. Introduction

Composite T-joints are commonly used in aerostructures for joining of composites, with typical applications including spar-to-skin and stiffener-to-skin interfaces in wing structures, as well as bulkhead-to-skin interfaces in the fuselage [1, 2]. ‘T’ structures are also found as stiffeners to prevent skin buckling in aerostructures. The flange of the T-joint interacts with the skin, whilst the web provides an attachment to the substructure. For such applications, tensile (pull-out) and flexural loads are representative of typical in-service loading conditions [2], and hence the tensile and flexural tests on T-joints are reported in the literature. In addition, the T-shaped composite structures were extensively studied for the civil engineering sector, with an emphasis on the out-of-plane mechanical behaviour, e.g. pull-out or bending, of pultruded [3-6] and adhesively bonded structures [7]. As most of the composite T-joints are subjected to out-of-

plane in-service loads, the catastrophic failure mode of delamination for laminates is commonly observed in laminated T-joints [8-10]. As a result, recent studies have investigated the benefits of adding through-thickness reinforcements to composite T-joints. This includes inserting z-pins, stitches or tufts into laminated structures, as well as using 3D integrally manufactured reinforcement in the T-joints.

The effects of adding z-pins into composite T-joints has been experimentally and numerically studied in [11-16]. The tensile pull-off tests were performed on composite T-joints with and without z-pins. Koh et al.[11-13] found that introducing z-pins can improve the ultimate failure strength and total energy absorption of the T-joints by a maximum of 75% and 600% respectively at a z-pin content level of 4% by volume. However this does not raise the initial stiffness and failure load. It was also shown that z-pins can improve the damage tolerance of composite T-joints with impact-induced cracks. The improvement in T-joint properties was attributed to improved delamination resistance by the bridging tractions across delamination cracks from the pins. It should be noted that the in-plane properties of the composites decrease with increase in z-pin volume content due to fibre damage resulting from the insertion process [17].

Tufting can also be used to reinforce laminated T-joints but this process is only suitable for dry preforms before liquid composite moulding. Cartié et al. [18] found the tufted T-joints had a ultimate strength twice that for T-joints without tufts under a tensile pull-off test, along with a higher total energy absorption. It was shown that delamination in tufted specimens was stopped by the tufting thread.

Yang et al. [19] studied the mechanical behaviour of 3D integrally braided T-stiffeners under tensile pull-off loading, in comparison with a 2D laminated alternative. They found that the 3D braided specimen did not show delamination at the junction region unlike the 2D specimen, and consequently the 3D braided T-stiffener achieved a large improvement in ultimate strength. They concluded this advantage benefited from the fibre architecture of the 3D braided T-stiffener which led to a uniform strain distribution at the junction region, instead of a severe stress concentration. However, 3D braided materials are highly interlaced textile structures exhibiting a high level of yarn crimp, and it is well understood that crimp reduces the in-plane mechanical properties.

Soden et al. [20] assessed the influence of variations in the through-thickness reinforcement of 3D woven composite T-shaped specimens on mechanical behaviour under in-plane tensile loading, in comparison with a similar 2D laminated composite. It was found that the initial failure load of 3D woven specimens was similar to the laminated specimen and not improved by the 3D woven fibre architecture; however the peak load and damage tolerance were significantly increased. Although weave variations in the 3D woven specimens were limited to the proportion of through-thickness yarns, significant differences were shown from the results. In general, the peak failure load increases with increasing level of through-thickness yarns. It was indicated by the authors that the weave variations affect the failure mode of the specimens but the relationship is complex.

In general, it has been shown that z-pining, tufting or using 3D textile preforms in composites are all effective methods to improve the properties of composite T-joints, especially for

suppressing delamination and improving damage tolerance. Without degrading in-plane properties as much as tufted, Z-pinned or braided composites due to fibre damage or a high level of crimp, 3D woven materials are of particular interest in this work. This paper is to examine the influence of fibre architecture of 3D woven composite T-joints on mechanical performance, as well as the benefits that 3D woven T-joints can offer over the equivalent 2D laminates. A quasi-static tensile pull-off test was selected in the presented work to evaluate the 3D woven T-joints, as this out-of-plane load case is one of the critical loading conditions for T-joint structures [2, 3, 9, 13, 19, 21, 22]. In addition, research to date has not addressed the mechanical performance of 3D woven composite T-joints under this loading case. However, the T-joints should also be fully evaluated under other possible in-service loading conditions [1, 4, 23] before application, and this is recommended for further work.

## 2. Materials

The two types of 3D woven T-joint preform in this study were manufactured by Sigmatech UK from Hexcel IM7 12K carbon fibre. Specimens were woven flat with pre-positioned bifurcations on a Jacquard machine and then folded into a T shape, although this would produce additional deformation on the folded preforms [24]. The preforms were based on a 3D orthogonal weave with the only variation at the junction. Fig.1 from x-ray micro computed tomography ( $\mu$ CT) shows the fibre architectures with the direction of weft yarns marked, illustrating type 2, where half of the weft yarns are crossing over the other half at the junction, in comparison with type 1.

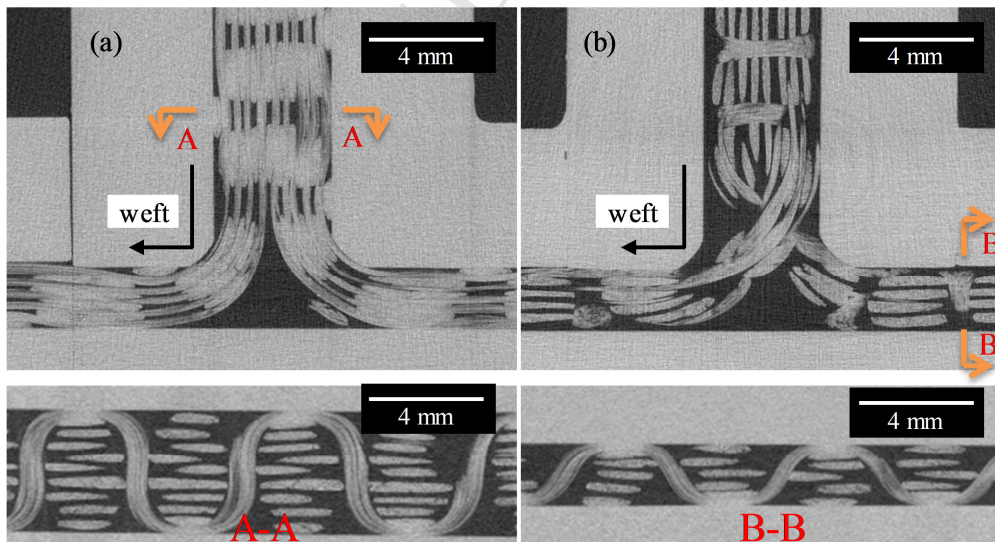


Fig. 1. Images from  $\mu$ CT scan of the two types of 3D preforms showing the weave variation at the junction: (a) type 1; (b) type 2; section views show the weave pattern (orthogonal) at web and flange

This weave variation was formed by opening different sheds when inserting the weft yarns at the junction, which consequently changed the path of weft yarns at the junction only. The schematic woven structures for the two types of 3D woven T-joint preforms highlighting the weave variation are presented in Fig. 2. Both 3D woven preforms consist of 8 layers of warp yarns and 9 layers of weft yarns in the web and 5 layers of warp yarn and 4 layers of weft yarns in the flange. More details of the  $\mu$ CT setup and the 3D woven preforms are given in [24].

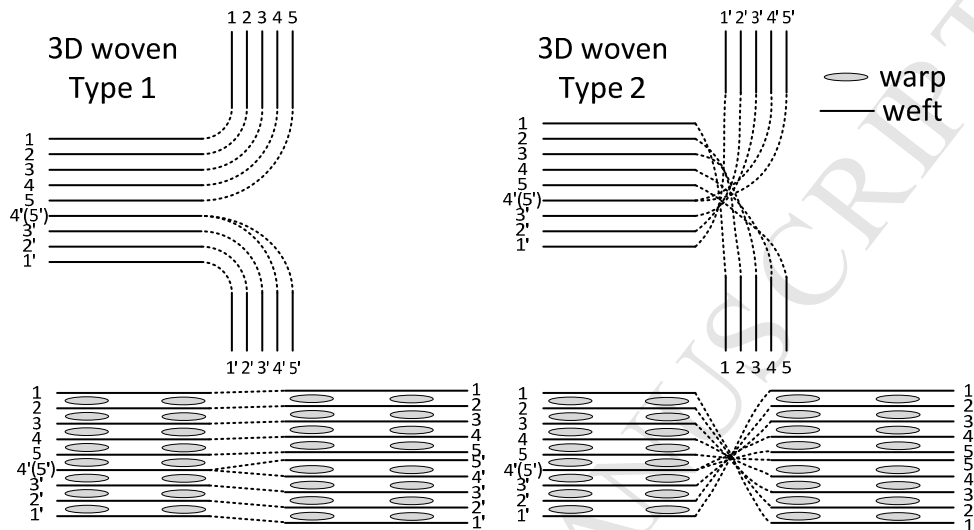


Fig. 2. Schematic woven structures for the two 3D preforms after (top) and before (bottom) bifurcation, showing the weave variation at the junction (dashed line area), with binders omitted

### 3. Fabrication of T-joint specimens

A vacuum assisted resin transfer moulding (RTM) process was used for manufacturing the composite T-joint specimens (Fig. 3). The 2D woven specimens for comparison are made of 6 layers of 2×2 twill weave Hexcel IM7 12K carbon fibre fabrics with an areal density of 660g/m<sup>2</sup>, infused with Gurit Prime 20LV epoxy resin, corresponding to a fibre volume fraction ( $V_f$ ) of 56% with thicknesses of 4mm in the web and 2mm in the flange. The two types of 3D woven composite T-joint specimen reinforced by the above preforms were moulded in the same way as the 2D woven specimen, giving a  $V_f$  of 45%, which is calculated based on the preform areal weight. One preform (approximately 170 mm in width) for each type of T-joint was moulded. The resin infusion, assisted by a vacuum, took 10 to 20 minutes at room temperature and then the specimens were cured in an oven at 50°C for 16 hours. It should be noted that 2D fabrics with suitable areal density to achieve a  $V_f$  of 45% were not available, resulting in a higher  $V_f$  for the 2D specimens.

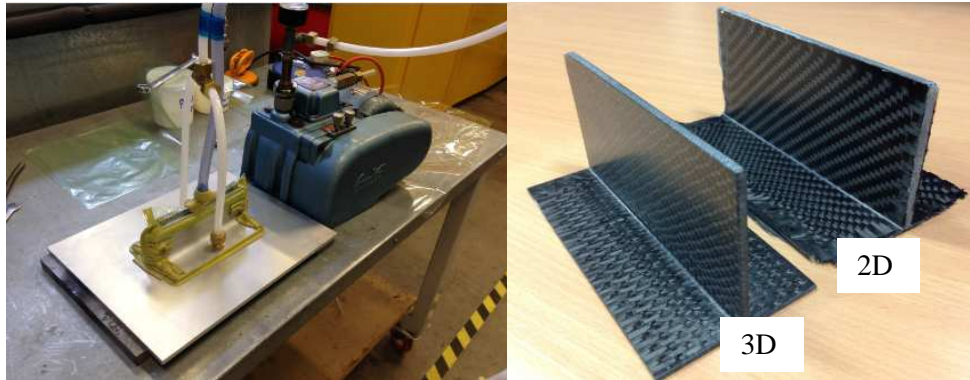


Fig. 3. Vacuum-assisted RTM process (left) and moulded specimens before cutting (right)

#### 4. Mechanical testing methodology

All three types of T-joint specimen were cut to the dimensions given in Fig.4 (left) and tested under quasi-static tensile pull-off loading. Using a 50kN Instron 5581 testing machine, a displacement load at a constant rate of 1 mm/min was applied on the web of the specimen, with the flange clamped at two ends by the fixtures shown in Fig.4 (right). The positions of the fixtures were adjusted to be symmetric with regard to the grip centre and bolted on the platform before testing, to ensure the specimens were properly positioned as shown in Fig.4 (left). A photo shows the testing layout for the composite T-joints are shown in Fig.4 (right). No tabs were used on the specimens but damage caused by grips was not observed. Testing continued after damage onset until the specimen fractured. Three specimens were tested for each of the 2D and two types of 3D woven T-joints respectively at constant room temperature, good consistency in load-displacement responses was observed for each type of the specimen (results for all specimens are given in Supplementary data and standard deviations are listed in Table 1). Specimens were painted on the front cross-sections before testing and a single-lens DANTEC Q400 Digital Image Correlation (DIC) system was used to monitor the full-field strains around the junction regions of all specimens.

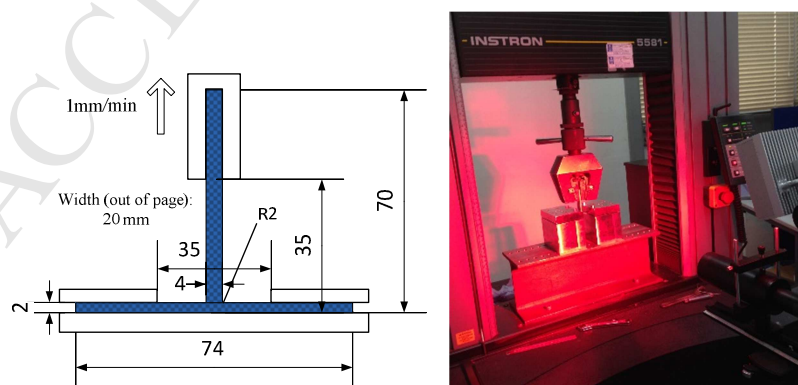


Fig. 4. Left, specimen dimensions (units: mm); right, testing layout for composite T-joints

## 5. Test results

### 5.1 Load-displacement responses

Load-displacement responses for the three types of composite T-joints (only one result of each tested T-joint type was displayed, refer to Supplementary data for complete results) under tensile loading are plotted in Fig.5. Both linear response in load-displacement curves at the beginning (displacement less than 0.1 mm) and stiffness degradation after that can be observed for the two 3D woven T-joints.

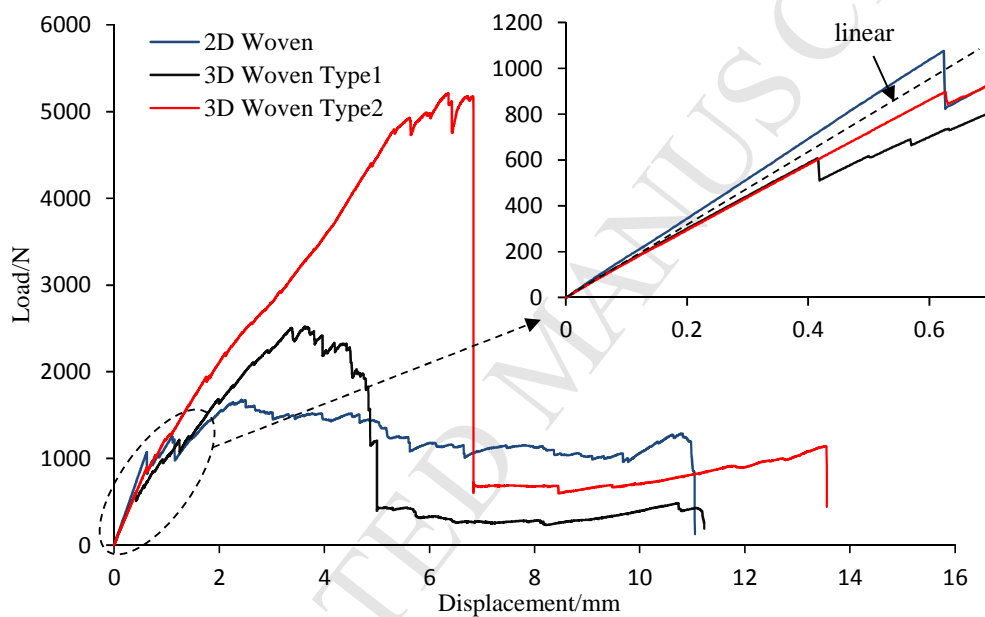


Fig. 5. Load-displacement responses for the three types of composite T-joints, with initial section of the curves enlarged shown on the top right, the dashed line in the top-right figure represents the initial linear stiffness of 3D woven T-joints

Each of the curves demonstrates the failure process of one typical T-joint, and can be divided into three stages in terms of the failure: 1) from the start of loading to the first load drop that represents the initial stiffness and failure onset of the T-joint; 2) from the first load drop to the peak load showing the ultimate strength of the structure; 3) from peak load to final failure load showing the final extension on the T-joints needed to completely fracture the structure.

## 5.2 Stiffness and damage initiation

The enlarged figure in Fig.5 shows the initial section of the curves that presents the initial failure load and stiffness of the structure. The stiffness at a displacement of 0.35 mm, initial and ultimate failure load and their standard deviations are compared in Table 1. Standard deviations were calculated based on the complete experimental data for all tested specimens. This shows that the 2D woven T-joint has the highest initial failure load at approximately 1128N, from where a significant load drop can be observed, as well as a higher initial stiffness. This can be attributed to the higher  $V_f$  in the 2D woven T-joint. Although the two types of 3D woven joints have the same  $V_f$ , the initial failure load and stiffness of the 3D woven type 2 specimen are respectively 37.7% and 6.5% higher than those of type 1, which results from the weave variation at the junction.

Table 1 Stiffness, initial and ultimate failure loads of the three types of specimen, with standard deviations in brackets

Specimen configuration	Stiffness at 0.35mm unit: N/mm	Initial failure load <sup>1</sup> unit: N	Ultimate failure load <sup>2</sup> unit: N	Displacement at ultimate failure unit: mm
2D woven	1627(±93)	1128(±44)	1620(±88)	2.3(±0.1)
3D Woven Type1	1378(±72)	710(±93)	2338(±152)	3.5(±0.2)
3D Woven Type2	1468(±32)	978(±59)	4951(±234)	5.9(±0.9)

<sup>1</sup> Initial failure load is defined at where a first significant load drop can be observed

<sup>2</sup> Ultimate failure load is defined at the maximum load

## 5.3 Ultimate strength and damage progression

3D woven composite T-joints show a significant improvement in energy absorption after damage initiation over the 2D woven T-joints in the tests. It is observed that the ultimate strength of the 3D woven type 1 specimens is improved by 44.3% over the 2D woven specimens, and the ultimate strength of the 3D woven type 2 specimens is 205.6% higher than that of the laminate as presented in Table 1. The non-linear behaviour of the composite T-joints is more evident after damage initiation. The 2D woven T-joints show a greater degradation in stiffness after damage initiation as well as a lower extension to failure than the 3D woven T-joints. This is partially explained by the absence of through-thickness reinforcement to arrest the propagation of damage. Moreover, the 3D woven type 2 specimens exhibit a higher post-failure stiffness than the 3D woven type 1 specimens. It is found that the weave variation alleviates strain concentration at the junction of 3D woven type 2 specimens to a large extent, as shown by strain distributions at a similar load after damage onset for the two types of 3D woven specimens in Fig.6.

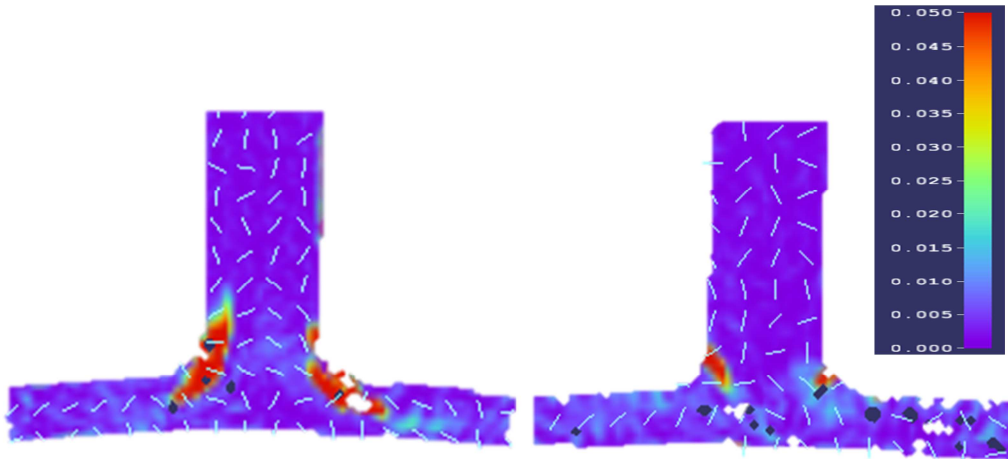


Fig. 6. DIC images showing maximum principal strain distributions of 3D woven type 1(left) and type 2(right) T-joints at a load of 1079N for (a) and 1089N for (b) respectively, with lines representing strain directions

#### 5.4 Characterisation of failure modes

Damage was initiated at the junction region of the three types of T-joint specimens and all tests ended by specimens rupturing at the edges of the clamps in the flange. Fig. 7 shows the failure propagation progress at the junction regions. For the 2D woven specimen, a thin crack in the yarn/matrix interface was observed when failure initially occurred, and increasing load caused several obvious cracks at the junction until it reached the ultimate strength. After that the T-joint can no longer withstand further loading and delamination propagated to the web and flange of the T-joint until fracture occurred at the clamps. The main failure mode for laminated T-joint structures is delamination which has been extensively investigated in previous studies [9, 25], and thus it is only briefly discussed in this work. Similarly, yarn/matrix interface damage shown in Fig. 7 (Stage 2), was observed to be the dominant failure mode for the 3D woven type 1 specimen. However, in Stage 3, in contrast to the 2D woven specimens, the binder yarns of 3D woven type 1 specimens at the junction limited the propagation of delamination into the web and flange which led to a higher ultimate strain. This comparison with the 2D woven specimen in terms of failure mechanism clearly demonstrates the effect of binder yarns in 3D woven composites on delamination resistance.

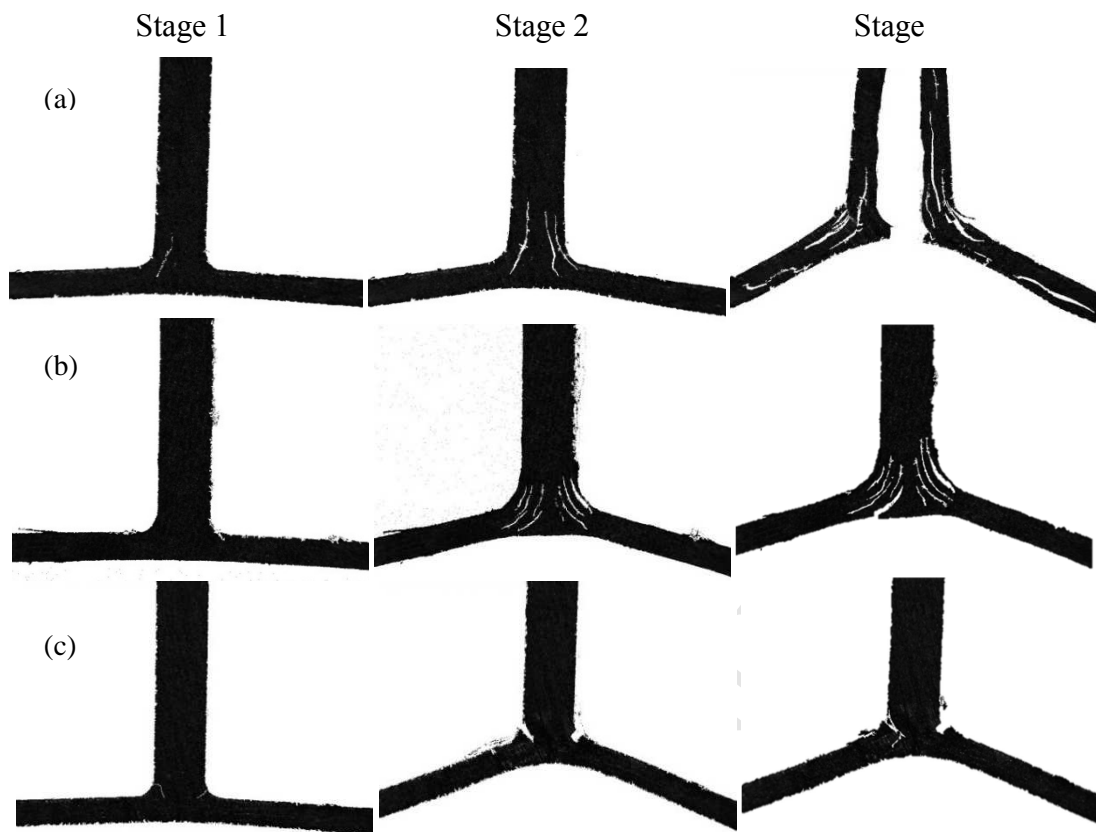


Fig. 7. Photographs taken by DIC camera during tests showing the damage at the end of each failure stage: (a) 2D woven; (b) 3D woven type 1; (c) 3D woven type 2

Post-mortem  $\mu$ CT scans were carried out to characterise the failure events inside the 3D woven T-joints. Fig. 8 shows the severe delamination at the yarn/matrix interfaces along with fibre fracture in binders and weft yarns experienced by the 3D woven type 1 specimen. Transverse cracking in warp yarns, fibre fracture in binders and weft yarns, and matrix cracking were also observed in the 3D woven type 2 specimen as shown in Fig. 9. Moreover, section views at A-A and B-B in Fig. 8 further demonstrate the effectiveness of binder yarns in restricting the propagation of delamination. Unfortunately, an accurate sequence of damage events is not available due to the lack of in-situ  $\mu$ CT scan during the tests.

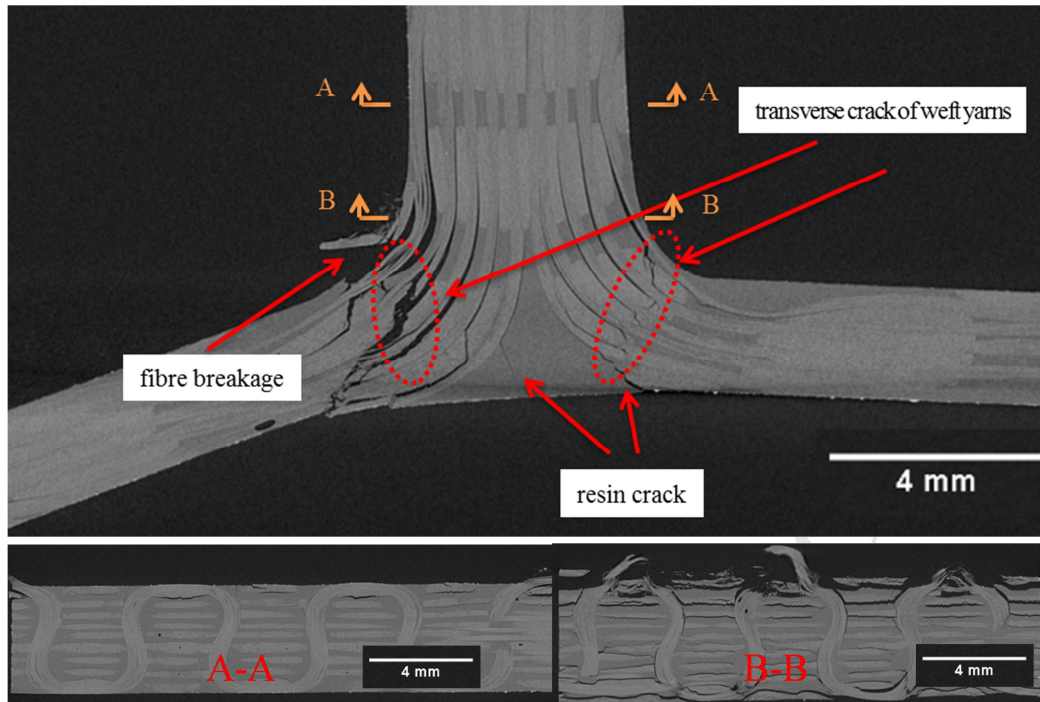


Fig. 8. Failure events in 3D woven type 1 T-joint specimen

The 3D woven type 2 T-joint specimen revealed a different failure mode in testing. As presented in Fig. 9, resin cracking was first observed at the fillets of the specimen, where two resin-rich regions were formed because of its weave pattern. After that the cracks grew until fractures occurred in the flange near the clamps. Minor delamination, transverse and fibre ruptures were observed in the  $\mu$ CT scan of the failed specimen.

Varying the weave pattern was found to change the failure mode of 3D woven T-joints which corresponds to a significantly different load-displacement response. It is also concluded from the experimental work that delamination in composite T-joints is a catastrophic failure mode, as the specimen without dramatic interfacial damage absorbs more energy than those that failed because of delamination. This experimental assessment demonstrates that using 3D woven reinforcements is an effective way to improve the damage tolerance of composite T-joints by reducing delamination under tensile pull-off loading, and also that this potential improvement could be optimised with regard to reinforcement fibre architecture.

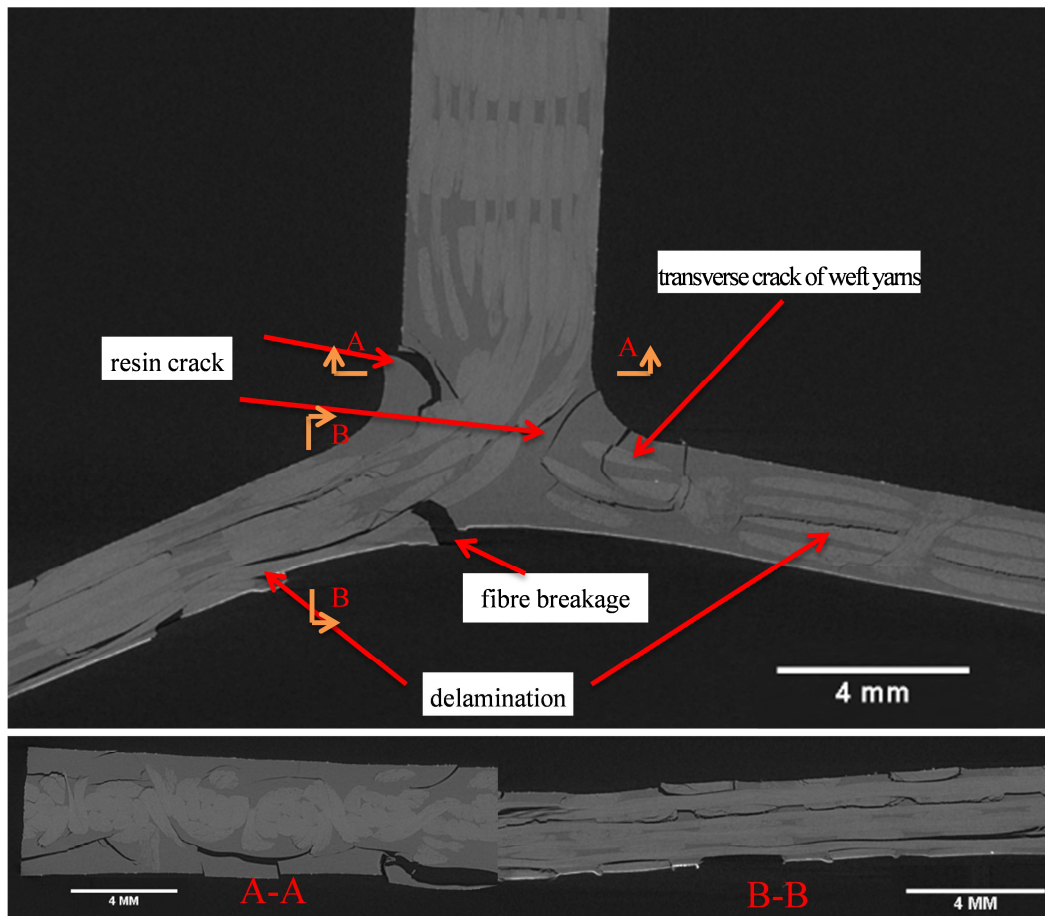


Fig. 9. Failure events in 3D woven type 2 T-joint specimen

## 6. Conclusions

The mechanical behaviour of two types of 3D woven T-joint with only weave variation at the junction were evaluated under a quasi-static tensile pull-off test, along with one type of 2D woven T-joint for comparison. All samples were made of carbon fibre/epoxy resin through a vacuum assisted RTM process. The advantages of 3D woven composite T-joints in terms of ultimate strength and damage tolerance over the 2D alternative were shown in the testing, although the 2D woven T-joint was found to have higher stiffness and initial failure load due to its higher fibre volume fraction. More importantly, this work showed that variation in the fibre architecture resulting from opening different sheds when inserting the weft yarns can considerably enhance properties such as delamination resistance, damage tolerance and total energy absorption to failure, as well as increasing slightly the stiffness and initial failure load. Whilst the fibre architectures are not directly comparable, it is noted that the higher strength (type 2) 3D woven specimen showed far greater improvement in ultimate failure load over 2D woven samples than observed in previous studies based on z-pinning and tufting. This experimental assessment has demonstrated that using 3D woven reinforcements is an effective way to improve the load-bearing capability of composite T-joints over laminates, and also that this improvement could be optimised with regard to fibre architecture.

## Acknowledgement

This work was supported by the Engineering and Physical Sciences Research Council (EPSRC), United Kingdom [grant number: EP/IO33513/1], through the EPSRC Centre for Innovative Manufacturing in Composites.

## References

- [1] Stickler PB, Ramulu M, Johnson PS. Experimental and numerical analysis of transverse stitched T-joints in bending. *Composite Structures*. 2000;50:17-27.
- [2] Stickler P, Ramulu M. Investigation of mechanical behavior of transverse stitched T-joints with PR520 resin in flexure and tension. *Composite Structures*. 2001;52:307-14.
- [3] Feo L, Mosallam AS, Penna R. Mechanical behavior of web-flange junctions of thin-walled pultruded I-profiles: An experimental and numerical evaluation. *Composites Part B: Engineering*. 2013;48:18-39.
- [4] Mosallam AS, Feo L, Elsadek A, Pul S, Penna R. Structural evaluation of axial and rotational flexibility and strength of web-flange junctions of open-web pultruded composites. *Composites Part B: Engineering*. 2014;66:311-27.
- [5] Fascetti A, Feo L, Nisticò N, Penna R. Web-flange behavior of pultruded GFRP I-beams: A lattice model for the interpretation of experimental results. *Composites Part B: Engineering*. 2016;100:257-69.
- [6] Quadrino A, Penna R, Feo L, Nisticò N. Mechanical characterization of pultruded elements: Fiber orientation influence vs web-flange junction local problem. Experimental and numerical tests. *Composites Part B: Engineering*. 2018;142:68-84.
- [7] Ascione F, Lamberti M, Razaqpur AG, Spadea S. Strength and stiffness of adhesively bonded GFRP beam-column moment resisting connections. *Composite Structures*. 2017;160:1248-57.
- [8] Phillips HJ, Sheno RA. Damage tolerance of laminated tee joints in FRP structures. *Composites Part A: Applied Science and Manufacturing*. 1998;29:465-78.
- [9] Hélénon F, Wisnom MR, Hallett SR, Trask RS. Numerical investigation into failure of laminated composite T-piece specimens under tensile loading. *Composites Part A: Applied Science and Manufacturing*. 2012;43:1017-27.
- [10] Hélénon F, Wisnom MR, Hallett SR, Trask RS. Investigation into failure of laminated composite T-piece specimens under bending loading. *Composites Part A: Applied Science and Manufacturing*. 2013;54:182-9.
- [11] Koh TM, Feih S, Mouritz AP. Experimental determination of the structural properties and strengthening mechanisms of z-pinned composite T-joints. *Composite Structures*. 2011;93:2222-30.
- [12] Koh TM, Feih S, Mouritz AP. Strengthening mechanics of thin and thick composite T-joints reinforced with z-pins. *Composites Part A: Applied Science and Manufacturing*. 2012;43:1308-17.
- [13] Koh TM, Isa MD, Feih S, Mouritz AP. Experimental assessment of the damage tolerance of z-pinned T-stiffened composite panels. *Composites Part B: Engineering*. 2013;44:620-7.
- [14] Bianchi F, Koh TM, Zhang X, Partridge IK, Mouritz AP. Finite element modelling of z-pinned composite T-joints. *Composites Science and Technology*. 2012;73:48-56.

- [15] Vazquez JT, Castanie B, Barrau JJ, Swiergiel N. Multi-level analysis of low-cost Z-pinned composite joints Part 2: Joint behaviour. *Composites Part a-Applied Science and Manufacturing*. 2011;42:2082-92.
- [16] Park YB, Lee BH, Kweon JH, Choi JH, Choi IH. The strength of composite bonded T-joints transversely reinforced by carbon pins. *Composite Structures*. 2012;94:625-34.
- [17] Mouritz AP. Review of z-pinned composite laminates. *Composites Part A: Applied Science and Manufacturing*. 2007;38:2383-97.
- [18] Cartié DDR, Dell'Anno G, Poulin E, Partridge IK. 3D reinforcement of stiffener-to-skin T-joints by Z-pinning and tufting. *Engineering Fracture Mechanics*. 2006;73:2532-40.
- [19] Yang QD, Rugg KL, Cox BN, Shaw MC. Failure in the junction region of T-stiffeners: 3D-braided vs. 2D tape laminate stiffeners. *International Journal of Solids and Structures*. 2003;40:1653-68.
- [20] Soden JA, Weissenbach G, Hill BJ. The design and fabrication of 3D multi-layer woven T-section reinforcements. *Composites Part A: Applied Science and Manufacturing*. 1999;30:213-20.
- [21] Burns L, Mouritz AP, Pook D, Feih S. Strengthening of composite T-joints using novel ply design approaches. *Composites Part B: Engineering*. 2016;88:73-84.
- [22] Li M, Chen P, Kong B, Peng T, Yao Z, Qiu X. Influences of thickness ratios of flange and skin of composite T-joints on the reinforcement effect of Z-pin. *Composites Part B: Engineering*. 2016;97:216-25.
- [23] Thomson RS, Falzon PJ, Nicolaidis A, Leong KH, Ishikawa T. The bending properties of integrally woven and unidirectional prepreg T-sections. *Composite Structures*. 1999;47:781-7.
- [24] Yan S, Zeng X, Brown L, Long A. Geometric modeling of 3D woven preforms in composite T-joints. *Textile Research Journal*. 2017;88:1862-75.
- [25] Trask RS, Hallett SR, Helenon FMM, Wisnom MR. Influence of process induced defects on the failure of composite T-joint specimens. *Composites Part A: Applied Science and Manufacturing*. 2012;43:748-57.